Journal of Hazardous Materials 496 (2025) 139272

Contents lists available at ScienceDirect

Journal of Hazardous Materials

journal homepage: www.elsevier.com/locate/jhazmat

Atmospheric transport of microplastics from land to sea is inefficient: Evidence from multimedia observations

Xiangrong Xu [a,*], Zhen Yuan [b,h], Yanxu Zhang [c], Hengxiang Li [d], Lang Lin [e], Shan Liu [a], Rui Hou [f], Eddy Y. Zeng [g]

[a] Guangxi Laboratory on the Study of Coral Reefs in the South China Sea, Coral Reef Research Center of China, School of Marine Sciences, Guangxi University, Nanning 530004, China
[b] Key Laboratory of Marine Mineral Resources, Ministry of Natural Resources, Guangzhou Marine Geological Survey, China Geological Survey, Guangzhou 511458, China
[c] Department of Earth and Environmental Sciences, Tulane University, New Orleans, LA, USA
[d] Key Laboratory of Tropical Marine Bio-resources and Ecology, Guangdong Provincial Key Laboratory of Applied Marine Biology, South China Sea Institute of Oceanology, Chinese Academy of Sciences, Guangzhou 510301, China
[e] South China Sea Sea Area and Island Center, Ministry Of Natural Resources (South China Sea Standard Measurement and Information Center, Ministry Of Natural Resources), Guangzhou 510310, China
[f] Guangdong Provincial Key Laboratory of Water Quality Improvement and Ecological Restoration for Watersheds, School of Ecology, Environment and Resources, Guangdong University of Technology, Guangzhou 510006, China
[g] Institute of Environmental Health, School of Environment and Energy, South China University of Technology, Guangzhou 510006, China
[h] University of Chinese Academy of Sciences, Beijing 100049, China

HIGHLIGHTS

- A year-long synchronized observation of AMPs on both land and sea was carried out.
- Microplastics are mainly fibers in cities, and the pollution level is closely related to population density.
- Only 1.8 % of the atmospheric microplastic emissions could be transported from land to sea.
- Atmospheric transport is not an efficient way to transport AMPs from land to sea.
- The treatment of marine MP pollution should first reduce riverine input.

GRAPHICAL ABSTRACT

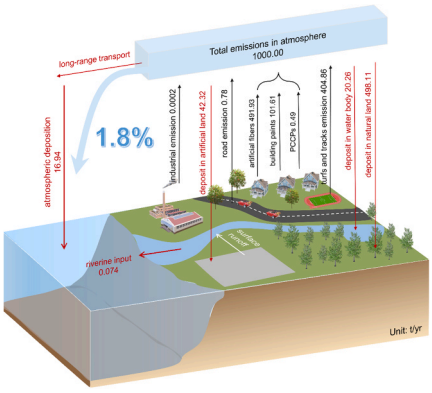

ARTICLE INFO

Keywords:
Microplastic pollution
Land-to-sea transport
Atmospheric transport

ABSTRACT

Microplastics have been recognized as a global marine environmental issue, but their sources, particularly the contribution of atmospheric transport, remain obscure. Here, we determine the transport efficiency of atmospheric microplastics (AMPs) from land to sea using multimedia observations from both sea and land in the South China Sea in conjunction with atmospheric trajectory modelling. Furthermore, we extrapolate AMP inputs to the

* Corresponding author.
E-mail address: xuxr@gxu.edu.cn (X. Xu).

https://doi.org/10.1016/j.jhazmat.2025.139272
Received 2 May 2025; Received in revised form 22 June 2025; Accepted 14 July 2025
Available online 23 July 2025

Deposition
Fiber

ocean at a global scale. The results show that only 1.8 % of AMPs are transported and deposited into the sea, with most remaining on land. The global mass of AMPs entering the sea is 262.98 t, which is much less than the river exports. Therefore, we conclude that the atmospheric transport is not the main pathway for land-sourced microplastics to enter the sea, and suggest that the foremost step of curbing the worsening of marine MP pollution is to control the inflow of riverine MPs into the sea.

1. Introduction

Misuse and mismanagement of plastic products have caused masses of plastic waste to accumulate in the environment and eventually enter in the oceans [1]. The potential annual transfer of plastic waste from land to the oceans is estimated to be 4.8–12.7 Mt [2], resulting in a global concern of plastic pollution. Understanding the sources, transport and fate of plastics is a prerequisite for reducing plastic pollution. Studies have initially recognized rivers as the main pathway for plastic debris to enter the oceans, but a growing number of studies are emphasizing the role of atmospheric transport, especially for microplastics (MPs, < 5 mm) [3–5]. There have been many reports on the presence of atmospheric microplastics (AMPs) in various regions [6–9], but the transport and environmental fate of AMPs are unknown.

Observations of AMPs in remote areas, such as the French Pyrenees Mountain [10], the Alps [11], the Tibetan Plateau [12] and polar regions [13], have demonstrated the long-range transport of AMPs; however, their land-to-sea transport and transport efficiency are rarely discussed and have not been properly quantified. Several scientists have preliminarily estimated the global transport mass of AMPs into the sea, but the estimates vary greatly and are not comparable, ranging from 10.02 t/yr to 100 kt/yr [4,14–16]. The proposed AMP transport efficiencies in these studies are also ambiguous, ranging from 1.8 % to 34 % [14,16]. The key to these large gaps seems to be the original dataset used in estimations. Limitations in monitoring methods make it difficult for a single team to conduct large-scale monitoring of AMPs on a national or global scale, so existing studies usually utilize literature data to develop estimates. On the one hand, the lack of global field data contributes to the high level of uncertainty in these estimates. More importantly, it is a great challenge to integrate the noncomparable datasets across regions and periods, because the monitoring methods for these datasets vary widely [17,18]. The absence of standardized monitoring procedures would directly lead to a high level of uncertainty in global extrapolation. For example, the pore size of sampling filters is critical to AMP abundance. A filter with a large pore size used in AMP collection may result in an underestimation of AMP abundance. For example, in a previous study done in France [10], if only AMPs with a size larger than 100 μm were counted, the AMP abundance was 36 ± 18 items/m^2/d, but if a wider range of AMPs (> 5 μm) were considered, the abundance increased to 365 ± 69 items/m^2/d. However, the pore size of filters used varied widely among studies, with a range from 0.45 to 100 μm [19–22], making it a challenge to describe the distribution of AMP pollution by comparing different studies. Besides, the differences in reported AMP abundances caused by inconsistencies in sampling or analytical methods can easily be misinterpreted as real differences in the environment, thereby reducing the reliability and credibility of the estimates.

Here, almost all our estimates of AMP land-to-sea transport were made using simultaneous observations to ensure the reliability of the original data and transport efficiency (the framework for this study is shown in Fig. S1). We conducted simultaneous observations in the South China Sea (SCS) and four Chinese coastal cities, with sampling consisting of both deposited and suspended AMPs (see Methods). Notably, our sampling project spanned 2021, and the same sampling methods and processing procedures were employed among all sampling sites, thereby preventing errors across seasons and methods. According to the year-round observations from Guangzhou and Xiamen in 2021, we confirmed the proportion of MPs entering the atmosphere and estimated the AMP emission in four Chinese coastal provinces (Guangxi, Guangdong, Fujian and Hainan) further using primary MP emission inventory established by Wang, et al. after adjusting the emission sources [23]. There are two potential pathways for AMPs to enter the sea, both of which were accounted for. The first is long-distance atmospheric transport, which was estimated using air trajectories and AMP emissions estimation. The second is riverine transport, as they can enter the sea after being deposited in rivers. The sum of the two pathways was the total mass of land-sourced AMPs entering the SCS, and the transport efficiency of AMPs from land to sea was calculated accordingly. These findings serve as a foundation for comprehending the fate of MPs in terms of their sources and sinks, as well as their global cycling.

2. Materials and methods

2.1. Study sites and sampling methods

Sampling sites on land were set in five representative cities, including Beihai (Guangxi Zhuang Autonomous Region), Guangzhou (Guangdong Province), Xiamen (Fujian Province), Sanya (Hainan Province) and Yongxing Island (belonging to Sansha, Hainan Province), as shown in Fig. S2. The sampling methods were consistent with what we did in Guangzhou before [24]. In 2021, total atmospheric deposition (including dry deposition and wet deposition) was simultaneously collected at monthly intervals in all five cities ($n = 72$) using passive samplers. Atmospheric deposition was dropped into a glass collection bottle via a stainless-steel funnel and obtained by filtration (Fig. S3). The collection bottle was placed inside a stainless-steel box to prevent the escape of fallout and contamination from ground dust. In addition, to estimate the proportion of MPs entering the atmosphere, suspended AMPs were monitored throughout 2021 in Xiamen and Guangzhou. A total of 171 samples were collected using middle-flow suspended particulate samplers, which were installed on the roofs of laboratory buildings. The samplers were set approximately 1.5 m above the floor, effectively avoiding resuspended ground dust. Sampling was generally performed every other day, with an intake flow rate of 100 L/min for 24 h.

Marine AMP samples from the SCS were obtained during a cruise in April 2022, with a navigation route map depicted in Fig. S2. A suspended particulate sampler was secured on the upwind area of the back deck (approximately 2.8 m above sea level) to collect suspended AMPs. The suspended particulate sampler and sampling procedures agreed with sampling in cities to verify the validity of the samples. A total of 20 sampling transects were set along the cruise and one sample was collected at each section. The detailed geographic information of sampling transects was presented in Table S1.

All samples were collected on glass microfiber filters (Whatman GF/A, 1.6 μm), and detailed sampling procedures can be found in our previous study [24]. All filters were kept in aluminum foil for further examination.

2.2. MP identification

A total of 263 filters were collected, including deposited AMP samples ($n = 191$, 171 samples collected on land and 20 samples collected above the sea) and suspended AMP samples ($n = 72$). Each filter was evenly divided into two (deposited AMP samples) or four equal parts (suspended AMP samples), and one was chosen as a representative sample at random. In total, 263 representative samples were randomly

selected, all of which were tested for MP identification.

Three steps were necessary for MP identification, including MP extraction, observation and identification. Firstly, according to the typical features of plastic materials (such as no biological or cellular structures, uniform color and shiny) [12,24], all suspected MPs were visually screened out under a stereoscopic microscope (Olympus SZX10, Japan). The filter should be scanned back and forth under the microscope from top to bottom at least four times to ensure that every corner of the filter has been examined. But due to the limitation of human eyesight (< 20 μm), MPs of extremely small size may be unnoticed. The characteristics of all suspected MPs were observed and recorded, including shapes, colors and sizes (length and width). The micro-Fourier transform infrared spectroscopy (FT-IR) technique was used for qualitative identification of all collected AMPs. The screened suspected MPs were carefully flattened and straightened one by one, and transferred subsequently to a clean and dry copper sheet with steel tweezers, keeping the MPs to be tested as close as possible to the copper sheet. To obtain spectra, the FT-IR spectrometers (Thermo Scientific Nicolet iN10, USA) scanned the suspected MP placed on the copper with a resolution of 4 cm^{-1} for 16 scans each in reflection mode. All obtained spectra were compared with the standard spectra library individually, and the polymer composition could be confirmed when the match was > 60 %, which is a widely accepted and applied ratio [15,20,24]. All suspected MPs screened out were tested. Based on the random sampling proportion, the final total number of MPs for a sample was determined to be double or four times the identified numbers. However, due to the distribution randomness of environmental samples, the final MP data were subject to 2–4 times uncertainty.

2.3. Quality assurance and quality control

Quality assurance control measures were taken during sampling and identification to minimize contamination and subjective errors. During sampling, to minimize potential contamination, all filters and glass supplies were baked at 450 ℃ in a muffle for 4 h, and rinsed water was filtered by microfiber filters (Whatman GF/A, 47 mm, 1.6 μm) before use. In addition, cotton lab coats and nitrile gloves were worn throughout the sampling and pretreatment processes to prevent contamination. Procedural blanks were made by placing an open, wet and pretreated filter during the filtration of atmospheric deposition. A total of 72 procedure blanks were obtained and they were taken back to the laboratory and analyzed along with the samples. No MPs were detected in the procedural blanks, but a few cotton microfibers were detected (detected in 2 of 72 blanks). Ropes were used to secure the equipment on the board, and observable ropes near the sampler on the board were collected and tested, but no comparable materials were discovered in marine AMP samples. To avoid subjective errors in recognizing MPs, MP identification for all samples was performed by the same experimenter in this study, including scanning suspected MPs under microscope and FT-IR analysis.

2.4. Total MP emissions

In this study, we estimated the total MP emissions from four coastal provinces of the SCS based on the primary MP emission inventory established by Wang, et al.[23]. According to the actual observations, we adjusted the emission inventory, and the final inventory included seven emission sources: clothing, architectural coating, automotive paints, road markings, plastic raw materials, artificial turfs and running tracks, personal care and cosmetics products, with rubber tires and marine coating removed (Text S1). The MP emissions from each source can be calculated by the following equation.

$$Emission = A \times EF \quad (1)$$

The calculations of activity (A) and emissions factors (EF_s) of each source were detained in Text S1. The annual MP emission fluxes of each city were determined independently, and most of the socioeconomic statistics used in the calculation were obtained from official data published by the National Bureau of Statistics of China in 2021.

A Monte Carlo simulation was performed to characterize the uncertainty of MP emissions. Uncertainty in related activity data and emissions factors are two major causes of the uncertainty in MP emissions (Table S2) [24], where EF has been listed directly in the formulas mentioned in Text S1, and the remaining factors in the fomulas are grouped into A. Twenty-eight parameters (both A and EF) from seven MP emission sources were entered into Crystal Ball software (Oracle). All inputs were randomly selected and the MP emissions were repeatedly calculated 10,000 times according to the Eq. (1). The activity (A) data and emissions factors (EF_s) were listed in Table S2. The model gave a prediction range of 12.80–549.00 kt for MP emission, taking the 90 % confidence interval as the uncertainty range for MP emissions (Fig. S9).

2.5. The proportion of MPs entering the atmosphere

Although total MP emissions are initially quantified, the fraction of MPs that become airborne is highly uncertain, with reported proportions ranging from 1 % to 40 % [16]. The proportion of MPs entering the atmosphere calculated based on literature data may deviate from the actual value due to differences in sampling methods and sampling periods. In this case, we determined the proportion (α) using annual synchronic AMP data from Guangzhou and Xiamen, as shown in the following formula.

$$\alpha = \frac{M_{AMPs}}{E_{MPs}} \quad (2)$$

where E_{MPs} is the total mass of MP emissions calculated based on the emission inventory in Text S1 and M_{AMPs} is the mass of AMPs, which can be defined as:

$$M_{AMPs} = \frac{A \times H}{T} \quad (3)$$

where A is AMP abundance, H is the height of the atmosphere (assuming that AMPs were well mixed over a range of 1000 m), and T is the atmospheric residence time of AMPs. According to all measured AMPs (N = 703), the predominant aerodynamic diameter range of AMPs was 50–90 μm, and the main polymer type was PET (1.38 g/cm^3). Therefore, PET with an intermediate diameter of 70 μm was chosen as representative AMP and used to calculate the unit mass of AMPs. Based on the size of AMPs, T was estimated to be between 3 and 28 h (detailed calculations can be found in Materials and methods 2.7). Here, we denote T as 24 h to make calculations easier.

The average annual abundance from Guangzhou was used to determine α, while the dataset from Xiamen was used for verification (Table S3). The resulting α was proven to be valid and feasible when the estimated mass matched the mass of AMPs calculated from the field observations.

2.6. AMP deposition in terrestrial environments

Population density is highly correlated with MP pollution levels [6,7], and it has been widely considered in MP emission estimates [2,25]. Combining our field data from five cities with data from Dongguan [26], we developed a regression model on population density (p) and MP deposition flux (Dep), as shown in the following equation (Fig. 1c):

$$Dep = 0.004p + 12.63 \quad (4)$$

The R-squared (R^2) of the regression model was 0.86, which implied that this model could simulate the variation of MP deposition flux as well. As a result, the AMP deposition flux could be inferred from this model for each city (Fig. S4), and the total MP deposition could be calculated by multiplying it by the city area. However, different land use

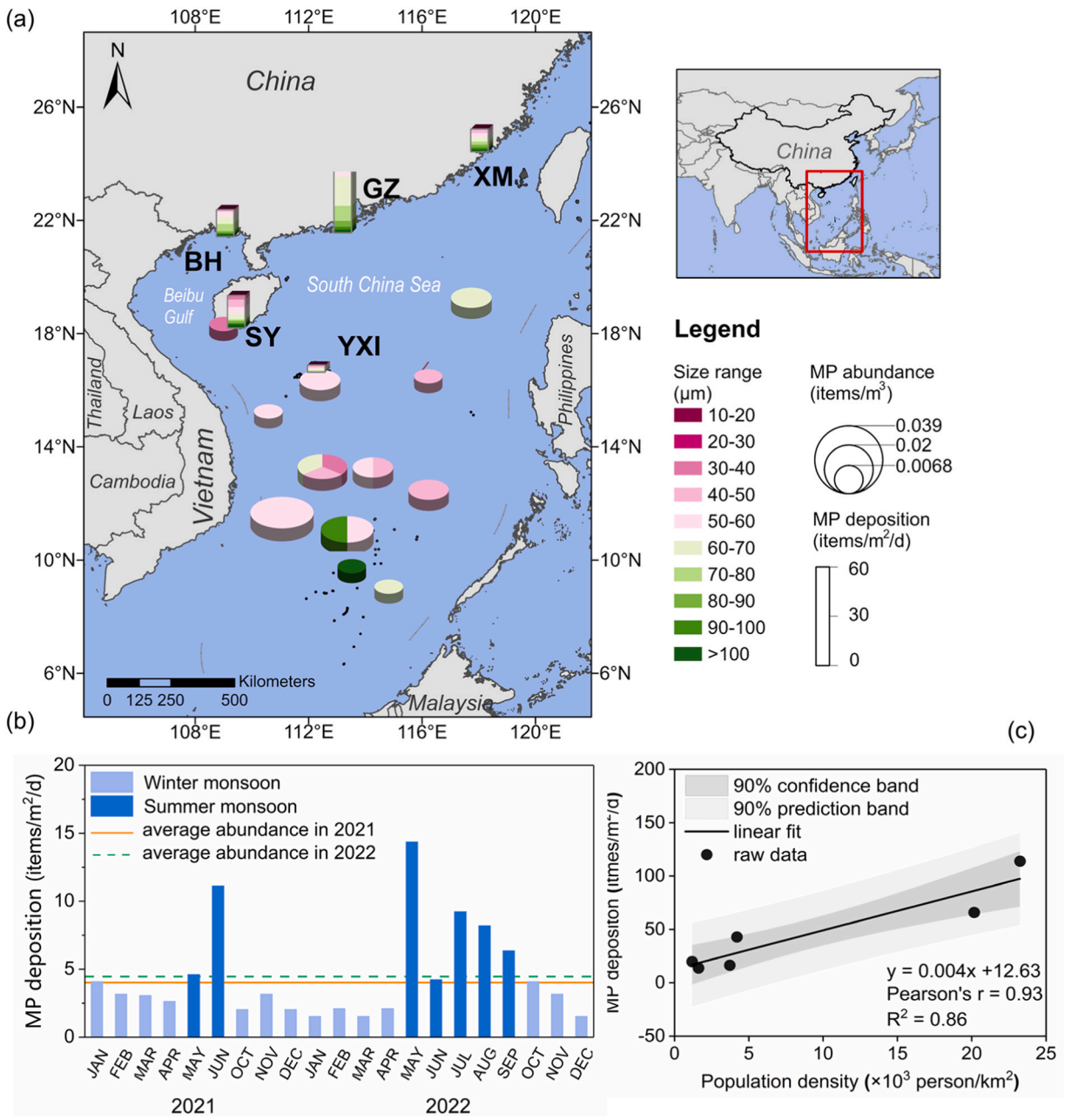

Fig. 1. AMP abundances in the South China Sea (SCS) region. The spatial distribution of AMP abundance (items/m^3), deposition fluxes (items/m^2/d) in the SCS region (including Beihai (BH) Guangzhou (GZ), Xiamen (XM) and Sanya (SY) and Yongxing Island (YXI)), aerodynamic size distribution (a) and AMP deposition at YXI from 2021 to 2022. The sampling on Yongxing Island in July, August and September of 2021 was interrupted due to a global pandemic of coronavirus disease 2019 and no data were obtained. Correlation between population density and AMP deposition (c), with one data from Huang, et al. and the rest were measured data from this work.

types where MPs are deposited may affect their fate. For example, AMPs deposited on artificial land could be washed into a water body via road runoff and then enter the ocean through river transport together with AMPs deposited directly into the water body [3,27,28]. Previous studies indicate that 6 % of AMPs can reach surface waters through road runoff [29,30]. The river transport probabilities of MPs from catchments to seas are suggested to be between 1.73–8.70 %, with an average value of 3.24 % for the top-ten catchments in Asia [31]. Therefore, the AMP deposition in each city was calculated separately for four land use types, including natural land (cultivated land, forest, grassland and semi-natural land), water bodies, artificial land and marine (Fig. S5). Land use data with a spatial resolution of 1 km were provided by the National Resources and Environment Database of the Chinese Academy of Sciences [32].

2.7. AMP transport trajectory model

The Hybrid Single-Particle Lagrangian Integrated Trajectory (HYSPLIT) model was applied to simulate the transport trajectory of air masses using Global Data Assimilation System (GDAS) meteorological data. Guangzhou was the most polluted site in study area (Fig. 2), so it was set as the starting point for the release of AMP pollution. The model was run in forward mode with a total run time of 28 h, starting at 100 m elevation above ground level (main altitude ranges of human activities). The model running time was determined by the maximum atmospheric residence time of AMPs, which was related to their aerodynamic

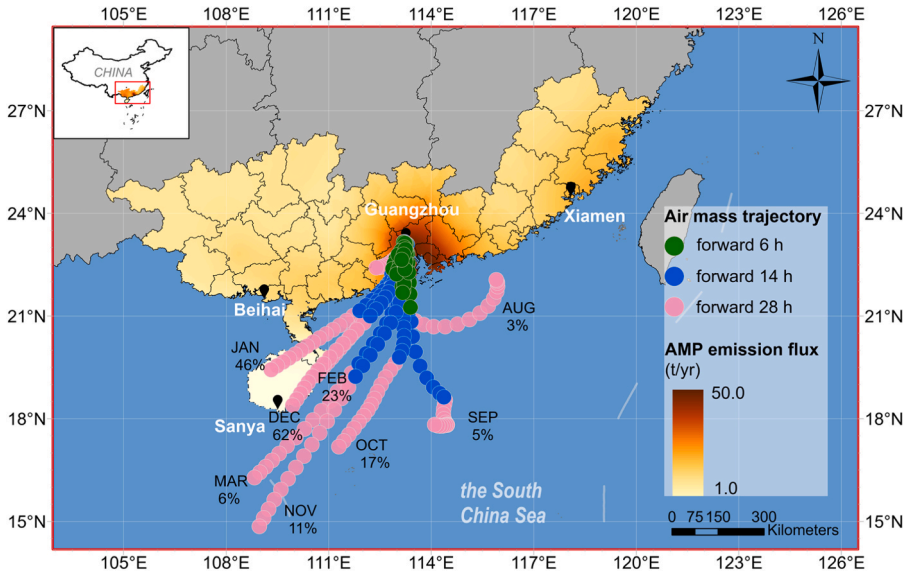

Fig. 2. Annual AMP emission for the four provinces adjacent to the South China Sea in 2021 and the distribution of seaward air masses according to forward trajectory modeling.

diameter. The atmospheric residence time and aerodynamic diameter could be calculated using the equations seen below [33,34].

$$D = \left(d_p \ln 2\theta\right)^{1/2} D_P \tag{5}$$

where D is the aerodynamic diameter, d_p is the density of plastics, θ is the aspect ratio of plastics and D_P is the cylindrical diameter of plastics.

$$V_t = \frac{gD^2\left(d_p - d_m\right)}{18\mu} \tag{6}$$

where V_t is the terminal velocity, g is the gravitational acceleration, D is the aerodynamic diameter, d_p is the density of plastics, d_m is the density of the air, and μ is the viscosity of air.

$$T = \frac{H}{V_t} \tag{7}$$

where T is the atmospheric residence time, and H is the height of air (assumed to be 1000 m).

The terminal velocity of AMPs followed a lognormal distribution (Fig. S6), and their 90 % confidence interval corresponded to an atmospheric residence time of 3–28 h. All trajectories were clustered at one-hour time intervals with a trajectory skip of 1 and analyzed for comparison by month.

Seaward trajectories were selected for further analyses (Fig. 2, approximately 15 % of a total of 7134 trajectories), and transport distances were calculated along the trajectory from the starting location to the deposition point. To ensure that most AMPs could reach the SCS, the transport distance should be at least 200 km, implying a 14 h atmospheric residence time. According to our measured size distribution of deposited AMPs (Fig. S6), only 11.3 % of AMPs met the conditions for a terminal velocity of less than 0.02 m/s and an atmospheric residence time over 14 h.

2.8. Data analysis

The Cystal Ball software (Oracle) was used to finish the Monte Carlo simulation, and Excel 2019 and SPSS 24.0 software (IBM, U.S.A.) were utilized for descriptive and statistical analysis. All analyses were carried out at a significance level of 0.05, and the data were reported as mean ± standard error (SE). A number of programs, including Origin 2022b, ArcGIS pro 2.8.6, and MATLAB R 2023a, were used to visualize the data.

3. Results and discussion

3.1. AMP abundance in the SCS region

Microplastics were widely present in all deposited samples, with deposition fluxes ranging from 4.11 to 109.34 items/m^2/d (Fig. S7a). For cities, the mean AMP deposition flux was significantly higher in Guangzhou (65.94 ± 7.53 items/m^2/d, Kruskal—Wallis test, $p < 0.05$), followed by Sanya (19.89 ± 3.19 items/m^2/d), Beihai (16.51 ± 2.88 items/m^2/d) and Xiamen (13.89 ± 1.83 items/m^2/d), as shown in Fig. 1a. However, there were no discernible differences in size distribution and shape between cities (see Supplementary Information for more AMP characteristics). The high AMP pollution level in Guangzhou may be because there were more AMP sources in densely populated cities with a high degree of anthropogenic activity [35,36]. The correlation analysis also confirmed a strong correlation between population density and AMP pollution (Pearson's correlation, $r = 0.93$, $p < 0.05$, Fig. 1c).

The two-year (from January 2021 to December 2022, Fig. 1b) AMP observations at Yongxing Island revealed that AMP deposition on islands far from land was markedly lower than that in cities, with an average deposition flux of 4.94 ± 0.83 items/m^2/d. Similarly, the analysis of marine air samples shown an average AMP abundance of 1.41 ± 0.23 items/100 m^3 in the SCS, which was obviously lower than our observations in cities, such as 0.17 ± 0.01 items/m^3 in Guangzhou and 0.07 ± 0.04 items/m^3 in Xiamen (detailed in Tables S1 and S3). As shown in Fig. 1a, AMP abundances were higher in the southwestern SCS, which may be attributed to emissions from neighboring Southeast Asian countries. The cruise occurred in April, and the SCS was in the summer wind period, so AMPs emitted from Southeast Asian land could be transported to the SCS by southwest winds (Fig. S8a), resulting in an increase in AMP abundance. These findings suggested a remarkable impact of land-based emissions on marine AMP distribution. The AMP abundance at Yongxing Island (1.40 items/100 m^3) was comparable to the mean (1.41 ± 0.23 items/100 m^3) and median values (1.39 items/100 m^3), according to our measured data during the cruise. Therefore, Yongxing Island was chosen as a representative site to calculate the total AMP deposition in the SCS. Based on the average AMP deposition flux at Yongxing Island, the total deposition of AMPs in the SCS was estimated to be 1.56 kt/yr (0.49–4.55 kt/yr) (Table S4).

3.2. Atmospheric MP emission

Our MP emission modelling revealed that a total of 166.61 kt MPs were discharged into the environment annually from four provinces adjacent to the SCS, with an uncertainty range of 12.80–549.00 kt (Fig. S9a). The estimation of primary MP emissions from seven sources was conducted by employing a range of socioeconomic data, such as population, residential area, and consumption of plastic products. Emission estimates were derived from the city level as the most basic unit, and 63 cities in Guangdong, Guangxi, Fujian and Hainan provinces were estimated. Synthetic fibers and artificial turfs accounted for approximately 90 % of MP emissions, which was compatible with our field observations that it was virtually all fibers (Text S2, Table S5). Synthetic fibers have long been recognized as a significant source of AMPs, and artificial turfs with a high nylon and polyethylene content have recently been proposed as an important source of AMPs [37,38].

Based on the MP emissions obtained previously and the field AMP data from Guangzhou and Xiamen, it has been defined that the fraction of MPs entering the atmosphere is 0.6 % (Table S3). Accordingly, a total of 1000.00 t AMPs were released annually into the atmosphere from the four provinces, with a distinct regional heterogeneity (Fig. 2). The Guangdong-Hongkong-Macao Greater Bay Area (GBA) is one of the most populous and rapidly developing areas in China, and MP contamination tends to be greater in densely urban agglomerations. The nine GBA cities in Guangdong Province were responsible for 67.5 % of Guangdong Province emissions and 33.2 % of total AMP emissions in the four provinces. These results indicated that the GBA is the most polluted area in the coastal regions of the SCS (Table S6). The high AMP abundances observed in GBA cities such as Guangzhou and Dongguan also demonstrate the high pollution level here [24,26,39]. Consequently, we reasonably considered Guangzhou as a center of AMP pollution and commenced the air mass projection from here.

3.3. The AMP budget

The direction of air mass flow and the residence time are the two most important determinants of whether AMPs can be transported to the sea. Due to the impact of monsoons, the seasonality of continental air pollution transport in Asia is pronounced [40,41]. Contaminated air masses can be only transported from mainland China to the SCS during the winter monsoon (northeastern winds) [42,43]. The air mass trajectories for each month in 2021 were acquired using the Hysplit forward trajectory model. Subsequent cluster analysis revealed that only 15 % of the air masses observed during this period exhibited a trajectory directed towards the sea (Fig. 2). On the other hand, a sufficiently long atmospheric residence time is necessary for AMPs to be effectively transported to the sea, which is constrained by their sizes. Only 11.3 % of AMPs could be transported over great distances and deposited in the SCS, according to the results of the size analysis. Therefore, it is estimated that 16.94 t AMPs could be transported through the atmosphere and deposited into the sea each year.

Some AMPs are deposited in response to precipitation or gravity [24,44]. A total of 560.69 t AMPs were deposited locally. Furthermore, the deposition was calculated for each of the four typical land use types, including natural land, artificial land, water bodies and marine (Fig. 3). The maximum deposition (498.11 t/yr) occurred on natural land due to the largest natural land area. The downward mobility of AMPs to groundwater is a complicated process, and the upper 25 cm of soil is regarded as a transient or persistent sink for MPs [45–47]. The potential contribution of groundwater to marine MP was therefore disregarded. Even in coastal areas, the area of the sea in the city is still very small and therefore the mass of AMPs directly deposited into the sea is negligible, weighing only 0.0004 t. Approximately 20.26 t AMPs settled annually into water bodies and entered the sea with rivers, which are the major pathway for MP transport into the seas [48,49]. On the other hand, approximately 42.32 t of AMPs were deposited on artificial land, a portion of which could be transported downstream by rivers after being washed into the water bodies [50]. As a result, the total mass of AMPs entering the sea through rivers was 0.74 t. We emphasize that this flux is for only the AMPs, not accounting for the MPs in the other environmental compartment. Therefore, this flux could not be directly comparable with the total riverine MP fluxes.

The remaining 422.05 t of AMPs were transported inland, with a low possibility of their eventual arrival in the ocean. Considering all pathways of AMPs to the sea, the ultimate input of AMPs from land to sea was 17.68 t. Our measurements in the SCS indicate that the sea received

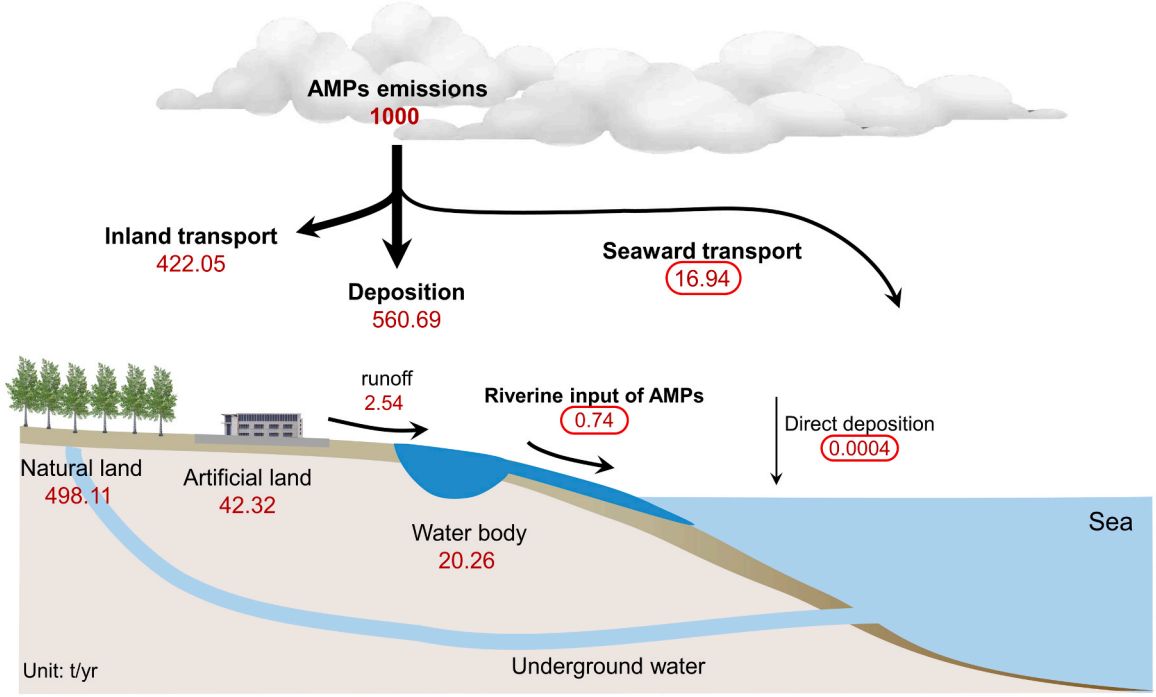

Fig. 3. Transfer fluxes for AMPs in four provinces adjacent to the SCS in China in 2021 (t/yr).

1.56 kt of AMPs deposition annually (Table S4), which come from all sources. It has demonstrated that our estimates of land-to-sea transport of AMPs are within an acceptable order of magnitude, since there is no question that any one source contributes less than the total deposition. This quantity represents a mere 1.8 % of the total AMP emissions, indicating that most AMPs tend to be retained on land. Moreover, for AMPs, the most of them enter the seas by atmospheric transport, with just a minor percentage sinking into the oceans with rivers following atmospheric deposition.

3.4. Land-to-sea transport of AMPs

The MP emissions from the four coastal provinces accounted for 23 % of the total MP emissions in China (737.29 Gg) [23], which could be considered the main contributor of MP emissions from mainland China to the SCS. However, China coasts may not be the primary source of AMPs in the SCS. This conclusion is reasonable and explainable. Our field observation in the SCS showed higher AMP abundance close to the coast of Southeast Asia, but almost none of the air masses along the coast of the SCS moved toward the sea in April (Fig. 2). Two years of AMP deposition monitoring in the SCS reveal that the summer months are a period of high AMP pollution, and at this time the winds are from the southwest. Slower summer winds extend the residence time of AMPs emitted from South Asian countries over the SCS and would favor AMP deposition. In contrast, winter winds are swift and short-lived, making it difficult to transport AMPs from mainland China into the sea (Fig. S8). On the other hand, countries bordering the SCS are also greatly affected by AMP pollution, especially Vietnam (172–292 items/m^2/d) [51], the Philippines (0.02 items/m^3) [52] and Malaysia (97–775 items/m^3) [53]. The estimation indicates that only approximately 1.1 % of the total deposition might originate from the four Chinese coastal provinces (Table S4), and more measured data from Southeast Asian countries are needed to completely clarify the source-sink of AMPs in the SCS.

We found a lower transport efficiency of AMPs from land to sea (17.68 t/yr, 1.8 % of the atmospheric emissions of MPs) compared to previous global studies, e.g., 21 % as proposed by Fu, et al. [4] and 34 % proposed by Evangeliou, et al. [16]. There are two possible reasons for these differences. First, these differences may be attributed to AMP emission estimates. Tire emissions were incorporated in previous emission estimates and are the greatest source, accounting for 84 % of the total [4,54]. However, the main component of tires is natural rubber, which is not listed in the ISO definition for plastics. Furthermore, tire wear particles are typically black fragments [55–57], but black did not make up a high percentage of observed particles in our observations, only roughly 11.7 %. Some black fragments were found only in the road dust and their polymer composition is not rubber or other tire additives [19,58], so the high 84 % share of tire emission need more supporting field data and further confirmation [5,54]. For the observed black particles, we matched their spectra to standard spectra library of rubber, resin and other common tire compounds, but the results were negative. Therefore, we excluded it from the MP emission inventory for the time being. The α of MPs entering the atmosphere is the most crucial factor in estimating AMP emissions. Long, et al. [54] suggested the α to be 12.5 % based on published AMP data; however, due to the fact that the data came from four research teams during 2016 and 2019, the results are greatly affected by the uncertainty of data integration across different teams and methodologies. On the basis of measured data from Guangzhou and Xiamen, we determined the α to be 0.6 % and ensured that the sampling method and processing procedures were completely consistent so that the resulting α is more reliable and conforms to reality. Notably, there is a possibility of overestimation, although our estimated α is much lower than the previous values. Our group conducted a vertical investigation of AMPs in 2021 and found that AMP abundance at 500 m was significantly lower than that at ground level [59]. Consequently, the assumption of uniform mixing of AMPs within the atmospheric boundary layer (set to 1000 m) in estimating the total mass of AMPs in Guangzhou and Xiamen may result in an exaggerated mass and an increased fraction of AMPs. The overestimated atmospheric transport efficiency of MPs is largely influenced by the high proportion of atmospheric emissions.

Another reason for the difference is the estimation of AMP deposition on land. Most studies estimated AMP deposition in their study areas based on published AMP deposition fluxes [14,21], but the comparability and availability of these data need to be validated. For instance, two research groups examined AMPs in Shanghai in 2018 and 2019, while the results differed by a factor of 200, with abundances of 1.42 $\pm$ 1.42 items/m^3 [60] and 267 $\pm$ 227 items/m^3 [7] respectively. Therefore, different choices of datasets could alter the estimated mass of AMPs deposited on land, potentially resulting in inflated atmospheric transport. To reduce data-related inaccuracies, we have standardized sampling and analytical procedures to ensure the availability of AMP data, and we have also used statistics from the same year as much as feasible. In addition to data errors, the mass calculation of MP is also a nonnegligible reason for differences. In previous studies, MPs were viewed as solid heterogeneous objects, and their mass was estimated by multiplying their polymer density by volumes [5,21,27,44]. MPs in actual environments may suffer density variations due to ageing and curling into hollow objects [61], leading to a large variance in overall mass. It is not yet known how much AMP mass is lost in the environment due to weathering or ageing; however, the conclusion that the atmospheric transport of MPs from land to sea is inefficient is unaffected.

The SCS has emerged as a hotspot for MP research [62,63], necessitating an urgent need to elucidate their origins. The Pasig River (Philippines), the Pearl River (China), and the Mekong River (Vietnam) are the major rivers that flow into the SCS and annually discharge 38.8 kt, 13.6 kt and 22.8 kt MPs into the sea, respectively [48]. The riverine input from any given river is considerably greater than the annual deposition of AMPs in the SCS (1.56 kt/yr), suggesting that atmospheric transport may be not the primary source of MPs in the SCS.

3.5. Uncertainty

The estimation of MP emissions is the basis of all further calculation, which is one source of uncertainty. Due to the uncertainties related to activity levels and emissions factors of MP sources, the estimated range of MP emissions is 12.80–549.00 kt (Fig. S9a). One aspect that is missing from our estimation is potential resuspension of deposited AMPs. Strong winds or turbulence may re-suspend previous deposited AMPs and allow them secondary transport [22,64]. However, there is currently no clear allocation factor between emission sources and resuspended sources of MPs, making it difficult to quantify the uncertainty in this part because of limitations imposed by research gaps. Another issue we need to mention and concern is the variability in the MP emission inventory. Synthetic fibers are the most prominent contributing source in our MP emission estimation, and while our field observations have confirmed this estimate, it is not set in stone. Urban planning and plastic emissions regulations will cause changes in MP emission inventory as well as AMP emissions, which need to be considered in further estimation in the future.

Another major source of uncertainty is the proportion of MPs entering the atmosphere. Values reported in the literature range from 1 % to 40 %, and some studies have even extended the upper limit to 83 % [16,54], which may not be conducive to further accurate estimation. Assuming that all MPs emitted into the air are deposited, and then estimate the corresponding α is 0.1 %–4.4 % using the AMP deposition calculated from measured data. Besides, based on the year-round AMP observations in Guangzhou, the α varies from 0.03 % to 1.5 % (Table S3). Combining these two results, the uncertainty range for α can be further narrowed to 0.1 %–1.5 %. It will be more scientific and accurate to confirm this ratio using a different dataset. However, we insisted on using synchronized measured data for estimation whenever possible, so the limitation of field data prevented us from further

validating.

We eventually estimate the uncertainty of our simulated AMP land-sea transport efficiency to be between 1.7 % and 7.5 %. Efficiency of land-sea transport of AMPs in different regions of the world ranged from 0.5 % to 40 %, with the South China Sea at about 2 % [16]. Our results are consistent with previous findings and give a finer range of AMP transport efficiency. It should be noted that the data used in our estimates are from coastal land, and therefore may be overestimated for inland areas far from the sea. More field studies are needed in the future, especially to complement the measured data from inland areas, to further understand the land-sea transport of AMPs.

3.6. Global Implications

We extrapolated our MP emission model and transport efficiency to the global level for a direct comparison between atmospheric transport and riverine input (Text S3). The annual global AMP emissions from land sources were estimated to be 14.61 kt, of which only 262.98 t (uncertainty range of 248.37–1095.76 t) could be deposited into the seas. This estimate is significantly lower in magnitude compared to earlier global estimates, such as the 13 kt/yr reported by Brahney, et al. [5] and 25 kt/yr reported by Fu, et al. [4]. The total annual global riverine emissions of plastics from land to sea are generally estimated to range from 0.1 to 1270 Mt [2,25,48,65], and the global export of MPs to the sea can also reach 47 kt per year [66]. We note that our worldwide estimation, which is based solely on field observations from the SCS region, is subject to considerable uncertainty. The 1.8 % land-to-sea transport efficiency should be used carefully, especially for inland areas with climates that differ significantly from the SCS, since AMP environmental fate will be directly impacted by variations in the weather. AMPs are supposed to have a poorer land-to-sea atmospheric transport efficiency than coastal areas due to the greater transport distances for inland locations from land to sea. Therefore, using the MP atmospheric transport efficiency from the SCS may lead to an overestimation of the land-sea transport in inland areas. But on the other hand, low precipitation in inland locations may result in less wet deposition of AMPs, which will increase the likelihood that the AMPs could be driven by the wind and travel long distance. However, there is still a lack of field observations to verify the final impact of the two effects mentioned above. On a global scale, population and plastic emissions tend to be concentrated in coastal regions [1]. From this perspective, the SCS region might be able to serve as a representative region, and the global extrapolated estimates based on these regional observations could be used as a reference value until more accurate observations are available. Despite the imperfection of our estimates, the huge order of magnitude difference between riverine input and atmospheric transport suggested that the riverine transport of MPs surpasses their atmospheric transport. The size of MPs may be the key to explaining the immense differences between atmospheric transport and riverine transport because larger plastic debris can float with rivers but cannot travel through the air. These results indicated that atmospheric transport is unlikely to be the primary channel for land-sourced MPs into the seas, and their land—sea transport efficiency is much lower than previously believed. We suggest that atmospheric transport may be not the main culprit for current serious marine MP pollution, and therefore the key to mitigating marine MP pollution depends on controlling and reducing riverine MP discharges to the seas.

Environmental Implication

Marine microplastic pollution is a serious and rapidly growing global problem that requires urgent action to reduce marine microplastics and their impacts. Clarifying the source of marine microplastics is a prerequisite for reducing microplastic pollution. For the first time, this study presents synchronized observations of atmospheric microplastics in five coastal cities throughout the year and determines the land-to-sea atmospheric transport efficiency of microplastics to be 1.8 % based on field data, which has been overstated in previous models. The findings provide valuable insights and scientific support for clarifying the source-sink of marine microplastics, with direct implications for future management strategies.

CRediT authorship contribution statement

Rui Hou: Software. **Eddy Y. Zeng:** Writing – review & editing. **Lang Lin:** Investigation. **Shan Liu:** Investigation. **Yanxu Zhang:** Writing – review & editing, Formal analysis. **Li Heng-Xiang:** Methodology, Investigation. **Xu Xiang-Rong:** Writing – review & editing, Project administration, Funding acquisition, Formal analysis, Conceptualization. **Zhen Yuan:** Writing – original draft, Visualization, Methodology, Investigation, Funding acquisition, Data curation.

Declaration of Competing Interest

The authors declare that they have no known competing financial interests or personal relationships that could have appeared to influence the work reported in this paper.

Acknowledgement

This work was supported by Guangxi Science and Technology Program (No. AD25069075), Hainan Province Science and Technology Special Fund (No. ZDYF2022SHFZ317), National Natural Science Foundation of China (No. U2005207), the Director General's Scientific Research Fund of Guangzhou Marine Geological Survey, China (No. 2024GMGS-QN-02). We thank Daning Li, Chang Chen, Zhenhua Long, and Fanyu Zheng of the Xisha Marine Science Comprehensive Experimental Station, South China Sea Institute of Oceanology, Chinese Academy of Sciences for their assistance. We acknowledge Prof. Minggang Cai from Xiamen University, Prof. Hongmei Jing from Institute of Deep-sea Science and Engineering, Chinese Academy of Sciences, Mr. Bin Li from Guangxi Mangrove Research Center and Mr. Liangming Wang from South China Sea Fisheries Research Institute, Chinese Academy of Fishery Sciences and other researchers involved in sample collection.

Appendix A. Supporting information

Supplementary data associated with this article can be found in the online version at doi:10.1016/j.jhazmat.2025.139272.

Data availability

Data will be made available on request.

References

[1] Lebreton, L., Andrady, A., 2019. Future scenarios of global plastic waste generation and disposal. Palgrave Commun 5 (1), 6.
[2] Jambeck, J.R., Geyer, R., Wilcox, C., Siegler, T.R., Perryman, M., Andrady, A., Narayan, R., Law, K.L., 2015. Plastic waste inputs from land into the ocean. Science 347 (6223), 768–771.
[3] Allen, D., Allen, S., Abbasi, S., Baker, A., Bergmann, M., Brahney, J., Butler, T., Duce, R.A., Eckhardt, S., Evangeliou, N., Jickells, T., Kanakidou, M., Kershaw, P., Laj, P., Levermore, J., Li, D., Liss, P., Liu, K., Mahowald, N., Masque, P., Materić, D., Mayes, A.G., McGinnity, P., Osvath, I., Prather, K.A., Prospero, J.M., Revell, L.E., Sander, S.G., Shim, W.J., Slade, J., Stein, A., Tarasova, O., Wright, S., 2022. Microplastics and nanoplastics in the marine-atmosphere environment. Nat Rev Earth Environ 3 (6), 393–405.
[4] Fu, Y., Pang, Q., Suo Lang Zhuo, G., Wu, P., Wang, Y., Mao, M., Yuan, Z., Xu, X., Liu, K., Wang, X., Li, D., Zhang, Y., 2023. Modeling atmospheric microplastic cycle by GEOS-Chem: An optimized estimation by a global dataset suggests likely 50 times lower ocean emissions. One Earth 6 (6), 705–714.
[5] Brahney, J., Mahowald, N., Prank, M., Cornwell, G., Klimont, Z., Matsui, H., Prather, K.A., 2021. Constraining the atmospheric limb of the plastic cycle. Proc Natl Acad Sci USA 118 (16), e2020719118.

[6] Perera, K., Ziajahromi, S., Bengtson Nash, S., Manage, P.M., Leusch, F.D.L., 2022. Airborne Microplastics in Indoor and Outdoor Environments of a Developing Country in South Asia: Abundance, Distribution, Morphology, and Possible Sources. Environ Sci Technol 56 (23), 16676–16685.

[7] Zhu, X., Huang, W., Fang, M., Liao, Z., Wang, Y., Xu, L., Mu, Q., Shi, C., Lu, C., Deng, H., Dahlgren, R., Shang, X., 2021. Airborne Microplastic Concentrations in Five Megacities of Northern and Southeast China. Environ Sci Technol 55 (19), 12871–12881.

[8] Roblin, B., Ryan, M., Vreugdenhil, A., Aherne, J., 2020. Ambient Atmospheric Deposition of Anthropogenic Microfibers and Microplastics on the Western Periphery of Europe (Ireland). Environ Sci Technol 54 (18), 11100–11108.

[9] Boucher, J.; Friot, D., Primary microplastics in the oceans: a global evaluation of sources. In IUCN Gland: Switzerland, 2017.

[10] Allen, S., Allen, D., Phoenix, V.R., Le Roux, G., Durántez Jiménez, P., Simonneau, A., Binet, S., Galop, D., 2019. Atmospheric transport and deposition of microplastics in a remote mountain catchment. Nat Geosci 12 (5), 339–344.

[11] Bergmann, M., Mutzel, S., Primpke, S., Tekman, M.B., Trachsel, J., Gerdts, G., 2019. White and wonderful? Microplastics prevail in snow from the Alps to the Arctic. Sci Adv 5 (8), eaax1157.

[12] Dong, H., Wang, L., Wang, X., Xu, L., Chen, M., Gong, P., Wang, C., 2021. Microplastics in a Remote Lake Basin of the Tibetan Plateau: Impacts of Atmospheric Transport and Glacial Melting. Environ Sci Technol 55 (19), 12951–12960.

[13] Mishra, A.K., Singh, J., Mishra, P.P., 2021. Microplastics in polar regions: An early warning to the world's pristine ecosystem. Sci Total Environ 784, 147149.

[14] Evangeliou, N., Tichý, O., Eckhardt, S., Zwaaftink, C.G., Brahney, J., 2022. Sources and fate of atmospheric microplastics revealed from inverse and dispersion modelling: From global emissions to deposition. J Hazard Mater 432, 128585.

[15] Liu, K., Wang, X., Song, Z., Wei, N., Ye, H., Cong, X., Zhao, L., Li, Y., Qu, L., Zhu, L., Zhang, F., Zong, C., Jiang, C., Li, D., 2020. Global inventory of atmospheric fibrous microplastics input into the ocean: An implication from the indoor origin. J Hazard Mater 400, 123223.

[16] Evangeliou, N., Grythe, H., Klimont, Z., Heyes, C., Eckhardt, S., Lopez-Aparicio, S., Stohl, A., 2020. Atmospheric transport is a major pathway of microplastics to remote regions. Nat Commun 11 (1), 3381.

[17] Zhang, Y., Kang, S., Allen, S., Allen, D., Gao, T., Sillanpää, M., 2020. Atmospheric microplastics: A review on current status and perspectives. EarthSci Rev 203, 103118.

[18] Yuan, Z., Li, H.-X., Lin, L., Pan, Y.-F., Liu, S., Hou, R., Xu, X.-R., 2022. Occurrence and human exposure risks of atmospheric microplastics: A review. Gondwana Res 108, 200–212.

[19] Yukioka, S., Tanaka, S., Nabetani, Y., Suzuki, Y., Ushijima, T., Fujii, S., Takada, H., Van Tran, Q., Singh, S., 2020. Occurrence and characteristics of microplastics in surface road dust in Kusatsu (Japan), Da Nang (Vietnam), and Kathmandu (Nepal). Environ Pollut 256, 113447.

[20] Liu, K., Wu, T., Wang, X., Song, Z., Zong, C., Wei, N., Li, D., 2019. Consistent Transport of Terrestrial Microplastics to the Ocean through Atmosphere. Environ Sci Technol 53 (18), 10612–10619.

[21] Brahney, J., Hallerud, M., Heim, E., Hahnenberger, M., Sukumaran, S., 2020. Plastic rain in protected areas of the United States. Science 368 (6496), 1257–1260.

[22] Zhang, Q., Zhao, Y., Du, F., Cai, H., Wang, G., Shi, H., 2020. Microplastic Fallout in Different Indoor Environments. Environ Sci Technol 54 (11), 6530–6539.

[23] Wang, T., Li, B., Zou, X., Wang, Y., Li, Y., Xu, Y., Mao, L., Zhang, C., Yu, W., 2019. Emission of primary microplastics in mainland China: Invisible but not negligible. Water Res 162, 214–224.

[24] Yuan, Z., Pei, C., Li, H., Lin, L., Liu, S., Hou, R., Liao, R., Xu, X., 2023. Atmospheric microplastics at a southern China metropolis: Occurrence, deposition flux, exposure risk and washout effect of rainfall. Sci Total Environ 869, 161839.

[25] Mai, L., Sun, X.-F., Xia, L.-L., Bao, L.-J., Liu, L.-Y., Zeng, E.Y., 2020. Global Riverine Plastic Outflows. Environ Sci Technol 54 (16), 10049–10056.

[26] Cai, L., Wang, J., Peng, J., Tan, Z., Zhan, Z., Tan, X., Chen, Q., 2017. Characteristic of microplastics in the atmospheric fallout from Dongguan city, China: preliminary research and first evidence. Environ Sci Pollut Res 24 (32), 24928–24935.

[27] Sonke, J.E., Koenig, A.M., Yakovenko, N., Hagelskjær, O., Margenat, H., Hansson, S.V., De Vleeschouwer, F., Magand, O., Le Roux, G., Thomas, J.L., 2022. A mass budget and box model of global plastics cycling, degradation and dispersal in the land-ocean-atmosphere system. Micro Nanoplastics 2 (1), 28.

[28] Werbowski, L.M., Gilbreath, A.N., Munno, K., Zhu, X., Grbic, J., Wu, T., Sutton, R., Sedlak, M.D., Deshpande, A.D., Rochman, C.M., 2021. Urban Stormwater Runoff: A Major Pathway for Anthropogenic Particles, Black Rubbery Fragments, and Other Types of Microplastics to Urban Receiving Waters. Environ Sci Technol Water 1 (6), 1420–1428.

[29] Clayer, F., Jartun, M., Buenaventura, N.T., Guerrero, J.-L., Lusher, A., 2021. Bypass of Booming Inputs of Urban and Sludge-Derived Microplastics in a Large Nordic Lake. Environ Sci Technol 55 (12), 7949–7958.

[30] Boucher, J., Faure, F., Pompini, O., Plummer, Z., Wieser, O., Felippe de Alencastro, L., 2019. Micro) plastic fluxes and stocks in Lake Geneva basin. TrAC TrAC Trends Anal Chem 112, 66–74.

[31] Schmidt, C., Krauth, T., Wagner, S., 2017. Export of Plastic Debris by Rivers into the Sea. Environ Sci Technol 51 (21), 12246–12253.

[32] Xu, X.; Liu, J.; Zhang, S.; Li, R.; Yan, C.; Wu, S., China's multi-period land use land cover remote sensing monitoring data set (CNLUCC). *Resource and Environment Data Cloud Platform: Beijing, China* 2018.

[33] Allen, S., Allen, D., Baladima, F., Phoenix, V.R., Thomas, J.L., Le Roux, G., Sonke, J.E., 2021. Evidence of free tropospheric and long-range transport of microplastic at Pic du Midi Observatory. Nat Commun 12 (1), 7242.

[34] Wright, S.L., Ulke, J., Font, A., Chan, K.L.A., Kelly, F.J., 2020. Atmospheric microplastic deposition in an urban environment and an evaluation of transport. Environ Int 136, 105411.

[35] Gonzalez-Pleiter, M., Edo, C., Aguilera, A., Viudez-Moreiras, D., Pulido-Reyes, G., Gonzalez-Toril, E., Osuna, S., de Diego-Castilla, G., Leganes, F., Fernandez-Pinas, F., Rosal, R., 2021. Occurrence and transport of microplastics sampled within and above the planetary boundary layer. Sci Total Environ 761, 143213.

[36] O'Brien, S., Okoffo, E.D., Rauert, C., O'Brien, J.W., Ribeiro, F., Burrows, S.D., Toapanta, T., Wang, X., Thomas, K.V., 2021. Quantification of selected microplastics in Australian urban road dust. J Hazard Mater 416, 125811.

[37] Cheng, H., Hu, Y., Reinhard, M., 2014. Environmental and Health Impacts of Artificial Turf: A Review. Environ Sci Technol 48 (4), 2114–2129.

[38] Mehmood, T., Peng, L., 2022. Polyethylene scaffold net and synthetic grass fragmentation: a source of microplastics in the atmosphere? J Hazard Mater 429, 128391.

[39] Huang, Y., He, T., Yan, M., Yang, L., Gong, H., Wang, W., Qing, X., Wang, J., 2021. Atmospheric transport and deposition of microplastics in a subtropical urban environment. J Hazard Mater 416, 126168.

[40] Lelieveld, J., Bourtsoukidis, E., Brühl, C., Fischer, H., Fuchs, H., Harder, H., Hofzumahaus, A., Holland, F., Marno, D., Neumaier, M., Pozzer, A., Schlager, H., Williams, J., Zahn, A., Ziereis, H., 2018. The South Asian monsoon—pollution pump and purifier. Science 361 (6399), 270–273.

[41] Tian, L., Li, J., Zhao, S., Tang, J., Li, J., Guo, H., Liu, X., Zhong, G., Xu, Y., Lin, T., Lyv, X., Chen, D., Li, K., Shen, J., Zhang, G., 2021. DDT, Chlordane, and Hexachlorobenzene in the Air of the Pearl River Delta Revisited: A Tale of Source, History, and Monsoon. Environ Sci Technol 55 (14), 9740–9749.

[42] Ou-Yang, C.-F., Hsieh, H.-C., Wang, S.-H., Lin, N.-H., Lee, C.-T., Sheu, G.-R., Wang, J.-L., 2013. Influence of Asian continental outflow on the regional background ozone level in northern South China Sea. Atmos Environ 78, 144–153.

[43] Jeong, J.I., Park, R.J., 2017. Winter monsoon variability and its impact on aerosol concentrations in East Asia. Environ Pollut 221, 285–292.

[44] Chen, Y., Niu, J., Xu, D., Zhang, M., Sun, K., Gao, B., 2023. Wet Deposition of Globally Transportable Microplastics (<25 μm) Hovering over the Megacity of Beijing. Environ Sci Technol 57 (30), 1152–11162.

[45] Gao, J., Pan, S., Li, P., Wang, L., Hou, R., Wu, W.-M., Luo, J., Hou, D., 2021. Vertical migration of microplastics in porous media: Multiple controlling factors under wet-dry cycling. J Hazard Mater 419, 126413.

[46] Koutnik, V.S., Leonard, J., Glasman, J.B., Brar, J., Koydemir, H.C., Novoselov, A., Bertel, R., Tseng, D., Ozcan, A., Ravi, S., Mohanty, S.K., 2022. Microplastics retained in stormwater control measures: Where do they come from and where do they go? Water Res 210, 118008.

[47] Waldschläger, K., Lechthaler, S., Stauch, G., Schüttrumpf, H., 2020. The way of microplastic through the environment – Application of the source-pathway-receptor model (review). Sci Total Environ 713, 136584.

[48] Lebreton, L.C.M., van der Zwet, J., Damsteeg, J.-W., Slat, B., Andrady, A., Reisser, J., 2017. River plastic emissions to the world's oceans. Nat Commun 8 (1), 15611.

[49] Meijer, L.J.J., van Emmerik, T., van der Ent, R., Schmidt, C., Lebreton, L., 2021. More than 1000 rivers account for 80% of global riverine plastic emissions into the ocean. Sci Adv 7 (18), eaaz5803.

[50] Wang, C., O'Connor, D., Wang, L., Wu, W.-M., Luo, J., Hou, D., 2022. Microplastics in urban runoff: Global occurrence and fate. Water Res 225, 119129.

[51] Truong, T.-N.-S., Strady, E., Kieu-Le, T.-C., Tran, Q.-V., Le, T.-M.-T., Thuong, Q.-T., 2021. Microplastic in atmospheric fallouts of a developing Southeast Asian megacity under tropical climate. Chemosphere 272, 129874.

[52] Romarate 2nd, R.A., Ancla, S.M.B., Patilan, D.M.M., Inocente, S.A.T., Pacilan, C.J. M., Sinco, A.L., Guihawan, J.Q., Capangpangan, R.Y., Lubguban, A.A., Bacosa, H. P., 2023. Breathing plastics in Metro Manila, Philippines: presence of suspended atmospheric microplastics in ambient air. Environ Sci Pollut Res 30 (18), 53662–53673.

[53] Afiq Daniel Azmi, M., Yasin, N.L.N.M., NorRuwaida, J., Hasnatul, A.H., Dewika, M., Sara, Y.Y., 2023. Analysis of suspended atmospheric microplastics size at different elevation in Universiti Teknologi Malaysia, Kuala Lumpur. IOP Conference Series Earth Environmental Science 1144 (1), 012009.

[54] Long, X., Fu, T.M., Yang, X., Tang, Y., Zheng, Y., Zhu, L., Shen, H., Ye, J., Wang, C., Wang, T., Li, B., 2022. Efficient Atmospheric Transport of Microplastics over Asia and Adjacent Oceans. Environ Sci Technol 56 (10), 6243–6252.

[55] Liu, C., Li, J., Zhang, Y., Wang, L., Deng, J., Gao, Y., Yu, L., Zhang, J., Sun, H., 2019. Widespread distribution of PET and PC microplastics in dust in urban China and their estimated human exposure. Environ Int 128, 116–124.

[56] Jia, Q., Duan, Y., Han, X., Sun, X., Munyaneza, J., Ma, J., Xiu, G., 2022. Atmospheric deposition of microplastics in the megalopolis (Shanghai) during rainy season: Characteristics, influence factors, and source. Sci Total Environ 847, 157609.

[57] Purwiyanto, A.I.S., Prartono, T., Riani, E., Naulita, Y., Cordova, M.R., Koropitan, A. F., 2022. The deposition of atmospheric microplastics in Jakarta-Indonesia: The coastal urban area. Mar Pollut Bull 174, 113195.

[58] Klein, M., Fischer, E.K., 2019. Microplastic abundance in atmospheric deposition within the Metropolitan area of Hamburg, Germany. Sci Total Environ 685, 96–103.

[59] Yuan, Z., Pei, C.-L., Li, H.-X., Lin, L., Hou, R., Liu, S., Zhang, K., Cai, M.-G., Xu, X.-R., 2023. Vertical distribution and transport of microplastics in the urban atmosphere: New insights from field observations. Sci Total Environ 895, 165190.

[60] Liu, K., Wang, X., Fang, T., Xu, P., Zhu, L., Li, D., 2019. Source and potential risk assessment of suspended atmospheric microplastics in Shanghai. Sci Total Environ 675, 462–471.
[61] Alimi, O.S., Claveau-Mallet, D., Lapointe, M., Biu, T., Liu, L., Hernandez, L.M., Bayen, S., Tufenkji, N., 2023. Effects of weathering on the properties and fate of secondary microplastics from a polystyrene single-use cup. J Hazard Mater 459, 131855.
[62] Cai, M., Liu, M., Qi, H., Cui, Y., Zhang, M., Huang, P., Wang, L., Xie, M., Li, Y., Wang, W., Ke, H., Liu, F., 2022. Transport of microplastics in the South China Sea: A review. Gondwana Res 108, 49–59.
[63] Matsushita, K., Uchiyama, Y., Takaura, N., Kosako, T., 2022. Fate of river-derived microplastics from the South China Sea: Sources to surrounding seas, shores, and abysses. Environ Pollut 308, 119631.
[64] Khodabakhshloo, N., Abbasi, S., Turner, A., 2023. Resuspension of microplastics and microrubbers in a semi-arid urban environment (Shiraz, Iran). Environ Pollut 316, 120575.
[65] Weiss, L., Ludwig, W., Heussner, S., Canals, M., Ghiglione, J.-F., Estournel, C., Constant, M., Kerhervé, P., 2021. The missing ocean plastic sink: Gone with the rivers. Science 373 (6550), 107–111.
[66] Van Wijnen, J., Ragas, A.M.J., Kroeze, C., 2019. Modelling global river export of microplastics to the marine environment: Sources and future trends. Sci Total Environ 673, 392–401.